Inorganic Chemistry

Article

pubs.acs.org/IC

Metal-to-Metal Charge Transfer in AWO_4 (A = Mg, Mn, Co, Ni, Cu, or Zn) Compounds with the Wolframite Structure

Swagata Dey, Rebecca A. Ricciardo, Heather L. Cuthbert, and Patrick M. Woodward*

Department of Chemistry and Biochemistry, The Ohio State University, 100 West 18th Avenue, Columbus, Ohio 43210-1185, United States

Supporting Information

ABSTRACT: Using a combination of UV−visible spectroscopy and electronic structure calculations, we have characterized the electronic structures and optical properties of AWO_4 (A = Mn, Co, Ni, Cu, Zn, or Mg) tungstates with the wolframite structure. In $MgWO_4$ and $ZnWO_4$, the lowest energy optical excitation is a ligand to metal charge transfer (LMCT) excitation from oxygen 2p nonbonding orbitals to antibonding W 5d orbitals. The energy of the LMCT transition in these two compounds is 3.95 eV for $ZnWO_4$ and 4.06 eV for $MgWO_4$. The charge transfer energies observed for the other compounds are significantly smaller, falling in the visible region of the spectrum and ranging from 2.3 to 3.0 eV. In these compounds, the partially occupied 3d orbitals of the A^{2+} ion act as the HOMO, rather than the O 2p orbitals. The lowest energy charge transfer excitation now becomes a metal-to-metal charge transfer (MMCT) excitation, where an electron is transferred from the occupied 3d orbitals of the A^{2+} ion to unoccupied antibonding W 5d states. The MMCT value for $CuWO_4$ of 2.31 eV is the lowest in this series due to distortions of the crystal structure driven by the d^9 configuration of the Cu^{2+} ion that lower the crystal symmetry to triclinic. The results of this study have important implications for the application of these and related materials as photocatalysts, photoanodes, pigments, and phosphors.

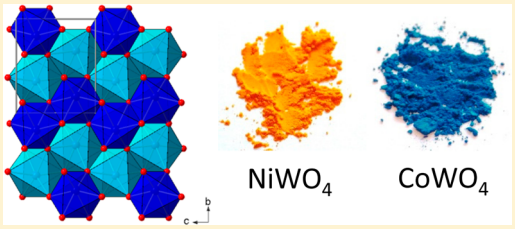

INTRODUCTION

First row transition metal tungstates of the AWO_4 type (A = Mn, Co, Ni, Cu, or Zn) have been widely studied for a range of applications. Compounds from this family have been used as heterogeneous catalysts,[1] for photoelectrochemical hydrogen gas production,[2,3] as photocatalysts for water splitting,[4−9] as multiferroic materials,[10,11] as humidity sensors,[12] as novel color pigments,[13] as phosphors,[14,15] and as photoanodes in either a photovoltaic electrochemical cell or a dye sensitized solar cell.[16,17] Five of these six AWO_4 compounds crystallize with the monoclinic wolframite structure.[18−24] The one exception is $CuWO_4$ where the Jahn−Teller type distortion of the local environment of the Cu^{2+} ion lowers the symmetry to triclinic.[25] Nevertheless the structure of $CuWO_4$ can be thought of as a distorted variant of the wolframite structure.

There are a variety of electronic excitations that can take place in these materials. The polyatomic WO_4^{2-} anion has a characteristic ligand to metal charge transfer (LMCT) transition that is at the heart of phosphors like $CaWO_4$. In this transition, an electron is transferred from the highest occupied molecular orbital (HOMO), which has oxygen 2p nonbonding orbital character, to the lowest unoccupied molecular orbital (LUMO), which is an antibonding orbital with W 5d orbital parentage. The tungsten environment in the wolframite structure is not the isolated tetrahedron found in $CaWO_4$; nevertheless, LMCT transitions are still an important contributor to the optical absorption of these compounds.[17,26] In addition, the presence of a cation with a partially filled set of d-orbitals, here Mn^{2+}, Co^{2+}, Ni^{2+}, or Cu^{2+}, leads to familiar d−d transitions. A third possibility is a transfer of electrons from the partially filled d-orbitals of the cation to the empty W 5d based molecular orbitals on the tungstate group. Because this effectively amounts to the transfer of an electron from the A^{2+} cation to the W(VI) ion, this transition can be labeled a metal to metal charge transfer (MMCT).

The variety of possible electronic transitions leads to considerable confusion in the literature when interpreting the optical properties, as will be discussed in this paper. For AWO_4 compounds where the A^{2+} ion is a closed shell ion (e.g., Sr^{2+}, Ca^{2+}, Mg^{2+}, Zn^{2+}, ...) both experimental measurements on single crystals[26,27] and calculations are available,[17,26] and the electronic transitions are well understood. However, when the A^{2+} ion is a transition metal with unpaired electrons (e.g., Mn^{2+}, Ni^{2+}, Cu^{2+}), the band gap decreases substantially, and the reasons for this are generally not well understood.[8] In some cases, the smaller size of the transition metal ions is invoked to explain the reduction in charge transfer energy,[27] but as shown here, the size of the A^{2+} in and of itself does not have a strong correlation to the energy and type of charge transfer transition. Calculations for AWO_4 compounds where A^{2+} is a paramagnetic transition metal ion are not so common, but Ruiz-Fuertes et al. have calculated a band gap of approximately 1.5 eV for $MnWO_4$.[26]

Received: December 31, 2013
Published: April 22, 2014

   dx.doi.org/10.1021/ic4031798 | Inorg. Chem. 2014, 53, 4394−4399

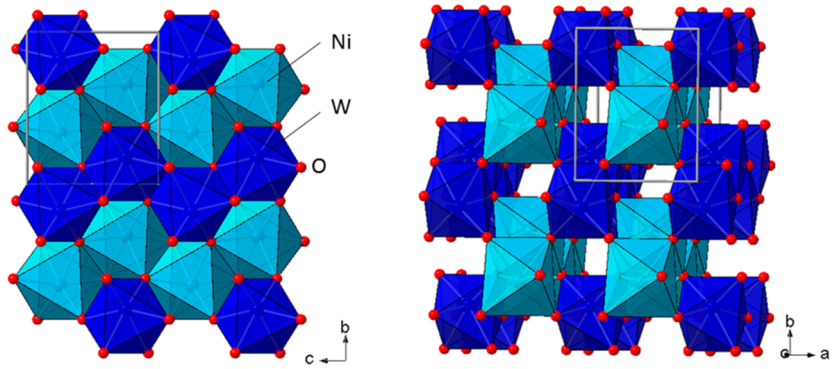

Figure 1. Two views of $NiWO_4$, which adopts the wolframite structure. The edge sharing chains are most evident when looking down the *a*-axis, as shown on the left, while corner sharing connectivity of neighboring chains can be more clearly seen looking down the *c*-axis, as shown on the right.

In this Article, we use experimental and computational methods to quantitatively characterize the electronic structures of tungstates with the wolframite structure. As we will show in this report, the band gap is more accurately described as a MMCT transition whenever the A^{2+} ion has partially filled d-orbitals (i.e., $MnWO_4$, $CoWO_4$, $NiWO_4$, and $CuWO_4$). By studying the entire family, we are able to develop a more accurate understanding of the electronic structure of this important family of compounds. This knowledge is key to designing improved catalysts, photocatalysts, pigments, and phosphors.

EXPERIMENTAL AND COMPUTATIONAL METHODS

Synthesis. Stoichiometric amounts of WO_3 (Alfa Aesar, 99.8%) and either CoO (Johnson Matthey, 99.9%), CuO (Baker, 99.5%), MgO (Allied Chemical, 98.5%), MnO (Cerac, 99.9%), NiO (Johnson Matthey, 99%), or ZnO (Alfa Aesar, 99.99%) were ground together in an agate mortar and pestle for 30 min, loaded into alumina crucibles, and heated to 900 °C in a box furnace for 8 h. Phase purity of the samples was confirmed using a Bruker D8 X-ray diffractometer equipped with a Cu anode and Lynx Eye detector. All patterns were matched with entries in International Center for Diffraction Data (ICDD) and verified using Jade (Version 8.5) software. In those cases where a single phase product did not form on the first heating, successive heating cycles and intermittent grindings were carried out until a phase pure product was obtained. X-ray powder diffraction patterns can be found in the Supporting Information.

Optical Properties. Diffuse reflectance spectra were collected with an Ocean Optics USB 4000 spectrometer equipped with a fiber optic reflectance probe and dual light source of deuterium and helium. A spectral range from 250 to 900 nm was probed. The reflectance data was then converted to absorbance data using the Kubelka–Munk transformation.[28,29] The optical band gap was extrapolated using Shapiro's method.[30]

Computational Methods. Geometry optimization and density of states calculations were performed using the Cambridge serial total energy (CASTEP) package. CASTEP is a first-principles density functional theory (DFT) program that uses a plane wave basis and pseudopotentials to model the potential felt by the electrons in the core region.[31] A Kerker scheme norm-conserving, nonlocal pseudopotential (energy cutoff = 380 eV) was employed. Each structure was geometry optimized by the BFGS scheme for subsequent analysis. An energy charge per atom convergence criterion of 5×10^{-6} eV was selected. Calculations were carried out on a $5 \times 4 \times 5$ Monkhorst–Pack grid of *k*-points. The generalized gradient approximation (GGA) and the Perdew–Burke–Ernzerhof (PBE) functional was used for the exchange and correlation effects.[32] The spin dependent option was chosen for all calculations on compounds containing unpaired d-electrons.

RESULTS AND DISCUSSION

In the wolframite structure, both the A^{2+} cation and tungsten ion are coordinated by six oxygen ligands in a highly distorted octahedral geometry. The W-centered octahedra form edge-sharing zigzag chains that run parallel to the *c*-axis, as do the A-centered octahedra. The two types of chains are connected to each other through corner sharing (Figure 1).

The structure of $CuWO_4$ is similar, but its symmetry is lowered to triclinic due a Jahn–Teller type distortion of the coordination environment of the d^9 Cu^{2+} ion.[25] Table 1 contains a summary of key structural parameters for each compound. Notice that the tungsten coordination is highly distorted from a regular octahedral geometry and the degree of distortion varies a little from one compound to the next, which is likely to have a subtle impact on the electronic structure and optical properties.

Table 1. Bond Distances for AWO_4 Compounds

	A–O distance (Å)	W–O distance (Å)	ref
$MgWO_4$	2.032 (×2)	1.783 (×2)	24
	2.121 (×2)	1.914 (×2)	
	2.157 (×2)	2.116 (×2)	
$MnWO_4$	2.081 (×2)	1.756 (×2)	21
	2.155 (×2)	1.937 (×2)	
	2.294 (×2)	2.157 (×2)	
$CoWO_4$	2.032 (×2)	1.785 (×2)	21
	2.121 (×2)	1.915 (×2)	
	2.157 (×2)	2.116 (×2)	
$NiWO_4$	1.994 (×2)	1.803 (×2)	21
	2.061 (×2)	1.956 (×2)	
	2.068 (×2)	2.107 (×2)	
$CuWO_4$	1.961, 1.967	1.760, 1.818	21
	1.978, 1.997	1.845, 1.988	
	2.347, 2.450	2.028, 2.200	
$ZnWO_4$	2.061 (×2)	1.816 (×2)	21
	2.133 (×2)	1.855 (×2)	
	2.139 (×2)	2.184 (×2)	

The colors of these tungstate salts are shown in Figure 2. $MnWO_4$ has a light buff color, $CoWO_4$ is blue, $NiWO_4$ is yellow, $CuWO_4$ is mustard yellow, and $ZnWO_4$ is white. The bright colors of $CoWO_4$ and $NiWO_4$ could be of interest for applications as pigments. It should be noted that salts containing Ni^{2+} are typically green, those containing Mn^{2+} are typically pale pink, and those containing Cu^{2+} are typically some shade of blue (e.g., the mineral azurite) or green (e.g., the

dx.doi.org/10.1021/ic4031798 | Inorg. Chem. 2014, 53, 4394–4399

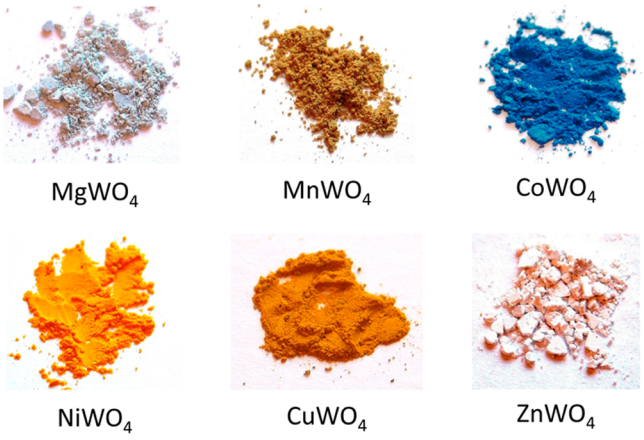

Figure 2. Colors of AWO_4 compounds.

mineral malachite) or a mixture of the two (e.g., the mineral turquoise). Hence the colors of these compounds are the first clue that electronic excitations other than d−d transitions are present in the visible region of the spectrum.

The UV−visible diffuse reflectance spectra of the six compounds studied are plotted together in Figure 3. The values have been converted to pseudoabsorbance spectra using the Kubelka−Munk transformation. The d−d transitions are assigned by comparing with $[A(H_2O)_6]^{2+}$ complexes of each A^{2+} ion in Table 2. In $MnWO_4$, the high spin d^5 configuration of the Mn^{2+} ion causes all of the d−d transitions to be spin forbidden, and thus only a very weak absorption peak is seen near 570 nm. This is quite close to the d−d transition observed at 2.22 eV (560 nm) in single crystals of $MnWO_4$.[27] In $CuWO_4$, a broad d−d transition occurs in the infrared region tailing into the visible. Its absorption maximum falls outside of the range of our spectrometer. This is a characteristic feature in the absorption spectra of Cu^{2+} salts that leads to absorption of low energy visible light (red, orange) and normally leads to a green or blue color. The mustard yellow color of $CuWO_4$ results from a combination of the d−d transition and a charge transfer transition that absorbs the photons that fall on the high energy side of the visible spectrum (λ < 535 nm). Both d−d transitions and charge transfer transitions are also found in the visible region of the spectrum for $CoWO_4$ and $NiWO_4$.

Table 2. UV−Visible−NIR Electronic Transitions for AWO_4 Salts

	d−d transitions (nm)	assignment[a]	onset of charge transfer (nm)	onset of charge transfer (eV)	assignment
$MnWO_4$	570	$^6A_{2g} \rightarrow {}^4T_{1g}$ (G)	455	2.72	Mn → W (MMCT)
$CoWO_4$	530	$^4T_{1g} \rightarrow {}^4T_{1g}$ (P)	465	2.67	Co → W (MMCT)
	600	$^4T_{1g} \rightarrow {}^4A_{2g}$			
$NiWO_4$	460	$^3A_{2g} \rightarrow {}^3T_{1g}$ (P)	415	2.99	Ni → W (MMCT)
	740	$^3A_{2g} \rightarrow {}^3T_{1g}$ (F)			
$CuWO_4$	850	$^2E_g \rightarrow {}^2T_{2g}$	536	2.31	Cu → W (MMCT)
$ZnWO_4$			315	3.95	O → W (LMCT)
$MgWO_4$			305	4.06	O → W (LMCT)

[a]The assignments were made by comparison to the d−d transitions in $[A(H_2O)_6]^{2+}$ given in ref 34.

Once we have accounted for the d−d transitions, we can rank order the six compounds from largest to smallest band gap (taken as the onset of charge transfer): $MgWO_4$ > $ZnWO_4$ > $NiWO_4$ > $MnWO_4$ > $CoWO_4$ > $CuWO_4$. Numerical values are given in Table 2. The values of the band gap energies for $MgWO_4$, $ZnWO_4$, and $CuWO_4$ are in excellent agreement with the values reported from absorbance measurements on single crystals: 4.06 eV for $MgWO_4$, 3.98 eV for $ZnWO_4$, and 2.3 eV for $CuWO_4$.[26,27] In contrast, our value of 2.72 eV for the band gap of $MnWO_4$ is 0.35 eV higher than the value of 2.37 eV reported in the literature.[26] The reason for this discrepancy is not clear, but there is no question that the onset of the charge transfer absorption in our sample of $MnWO_4$ falls at a higher energy than that reported in ref 26. Zawawi et al. reported a value of 2.97 eV for $NiWO_4$, which is in good agreement with our value.[8] Naik et al. reported a value of 2.95 eV for $CoWO_4$,

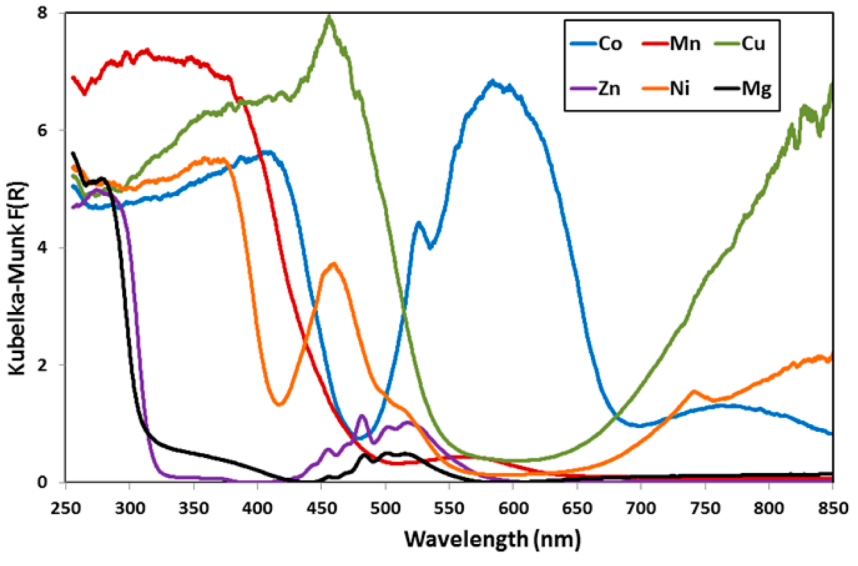

Figure 3. Reflectance spectra of AWO_4 compounds converted to absorbance using the Kubelka−Monk function.

dx.doi.org/10.1021/ic4031798 | Inorg. Chem. 2014, 53, 4394−4399

which is approximately 0.3 eV higher than our value. However, that study also reported a value of 2.79 eV for $CuWO_4$, which is substantially higher than our value as well as the single crystal value.[33]

$MgWO_4$ and $ZnWO_4$ do not have d−d transitions, and in contrast to the other compounds investigated here, their charge transfer excitations are located in the UV region of the spectrum. In $MgWO_4$, the onset of charge transfer excitation occurs at 305 nm and can be unambiguously assigned as a ligand to metal charge transfer (LMCT) transition from the filled oxygen 2p states to empty states that have predominantly W 5d character. The fact that the charge transfer excitation occurs at a similar value in $ZnWO_4$ indicates that the charge transfer in that compound is also a LMCT transition. The weak feature near 500 nm seen in the spectrum of $MgWO_4$ in Figure 3 is thought to be due to photoluminescence,[35] which appears as an absorbance in our reflectance spectrometer.

The UV−visible−NIR spectra of $MgWO_4$ and $MnWO_4$ are plotted on the same scale in Figure 4. Because the d−d

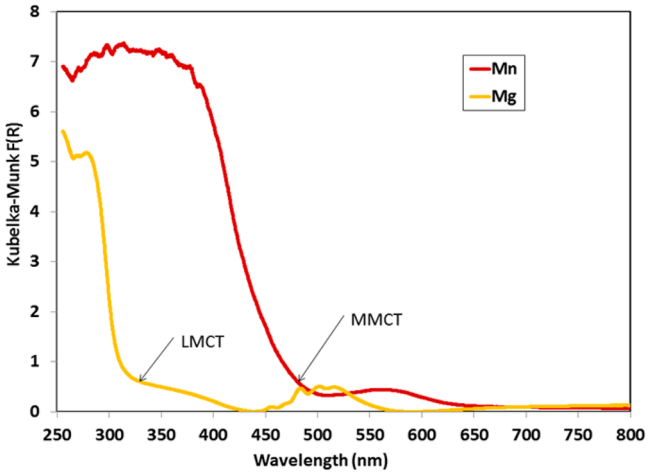

Figure 4. Reflectance spectra of $MgWO_4$ (red) and $MnWO_4$ (yellow) converted to pseudoabsorbance using the Kubelka−Monk function.

transitions in $MnWO_4$ are spin forbidden and rather weak, we can directly compare charge transfer excitations in both compounds. In $MgWO_4$, the onset of charge transfer occurs at 305 nm (4.06 eV), while in $MnWO_4$, the charge transfer energy is much smaller, 455 nm (2.72 eV). Because the geometry of the W-centered octahedron is fairly similar for both compounds (Table 1), it is not reasonable to expect such a large change in the energy of the LMCT transition. Instead we hypothesize that the charge transfer here is of a different type. The charge transfer seen in $MnWO_4$ is associated with the excitations from crystal orbitals that are partially filled and predominantly Mn 3d in character to crystal orbitals that are empty and predominantly W 5d in character. This transition can be labeled a metal to metal charge transfer (MMCT) transition. Implicit in this assignment is the fact that the O 2p orbitals are strongly hybridized with the W 5d orbitals and to a lesser extent with the Mn 3d orbitals.

To confirm our hypothesis of a MMCT transition in $MnWO_4$, we carried out band structure calculations on $MgWO_4$ and $MnWO_4$. The density of states plot for $MgWO_4$ is shown in Figure 5. As can be seen from the partial density of states (PDOS) curves, the oxygen 2p orbitals make the dominant contribution to the filled bands located between 0

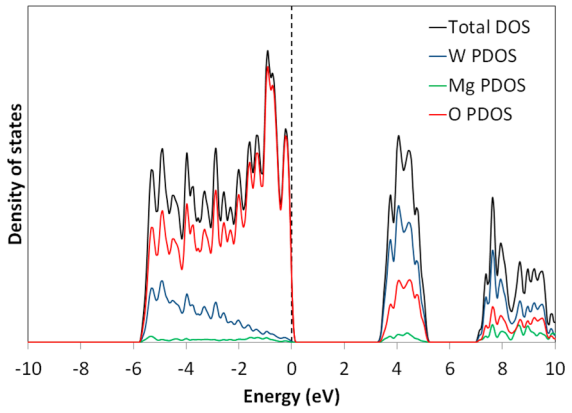

Figure 5. Density of states for $MgWO_4$. The Fermi energy is shown with a dashed line.

and −6 eV. The lowest energy set of unoccupied bands is centered at +4.3 eV. These bands have antibonding W 5d−O 2p orbital character. If we approximate the tungsten coordination to be octahedral, these bands can be described as originating from the t_{2g} set of W 5d orbitals. Inspection of the band structure diagram confirms that there are six bands in this energy range, which is exactly as would be expected for the triply degenerate t_{2g} set of bands, given the fact that there are two tungsten atoms per unit cell. It should be kept in mind that the tungsten environment is actually highly distorted from a perfect octahedron and the t_{2g} description is a crude approximation. Nevertheless, the lowest energy optical excitation in $MgWO_4$ can be described as a LMCT transition from the filled O 2p states to the empty W 5d states. The calculated band gap is 3.6 eV, which is in reasonably good agreement with the experimental value of 4.0 eV, as well as earlier calculated values of 3.48[17] and 3.22 eV.[26]

The PDOS plots for $MnWO_4$ are shown in Figure 6. Due to the presence of unpaired electrons on the Mn^{2+} ion, spin dependent calculations have been used. If we examine the DOS plot for $MnWO_4$, we find the same sets of bands as those seen in $MgWO_4$: the O 2p bands are now located approximately between −2 and −8 eV, and the t_{2g} set of W 5d bands are centered near +2 eV. In addition, we see two new peaks in the DOS that lie above the O 2p bands but below the Fermi level. The Mn PDOS plot shows clearly that the "extra bands" seen in $MnWO_4$ come predominantly from the Mn 3d orbitals. If we approximate the coordination environment of Mn^{2+} as an octahedron, we can assign these two peaks in the DOS as the Mn t_{2g} (centered at −2 eV) and Mn e_g (centered at −1 eV) bands.

To add further support for the presence of a MMCT at 2.7 eV in $MnWO_4$, consider the calculated energies of the LMCT and MMCT transitions. The energy of the LMCT transition corresponds to the energy separation between the top of the O 2p set of bands and the W 5d set of bands. This value is calculated to be approximately 3.7 eV in $MnWO_4$, which is very similar to the value calculated for $MgWO_4$. Thus, we can rule out the possibility that the energy of the LMCT transition is dramatically smaller in $MnWO_4$ than it is in $MgWO_4$. The energy separation between the DOS peak associated with the Mn 3d pseudo-t_{2g} set of bands and the W 5d set of bands is 2.4 eV, which is in reasonably good agreement with the experimental value of 2.7 eV. The energy separation between the Mn 3d pseudo-e_g set of bands is approximately 1.0 eV,

dx.doi.org/10.1021/ic4031798 | Inorg. Chem. 2014, 53, 4394−4399

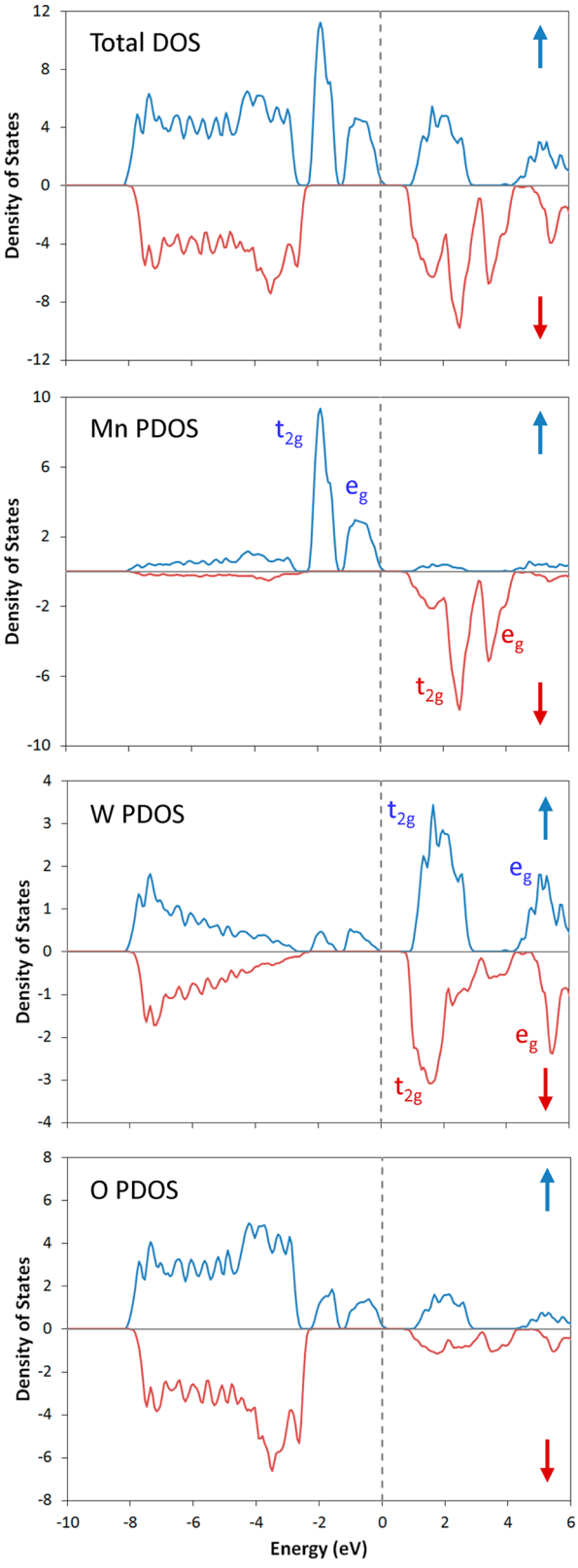

Figure 6. Total and partial density of states (DOS) plots for $MnWO_4$. The up-spin DOS is plotted above the *x*-axis, and the down-spin DOS below the *x*-axis. The Fermi energy is shown as a dashed line.

which is much smaller than the experimental value. This allows us to confidently assign the lowest energy charge transfer in $MnWO_4$ as a MMCT, from Mn 3d pseudo-t_{2g} states to empty W 5d states.

Similar inferences about the nature of MMCT can be drawn for $CoWO_4$, $NiWO_4$, and $CuWO_4$. The experimental charge transfer energies for all compounds studied are given in Table 2. For those compounds where the A^{2+} ion possesses partially filled 3d orbitals, the charge transfer energy can be assigned as a MMCT transition. The values for $MnWO_4$, $CoWO_4$, and $NiWO_4$ all fall in a relatively narrow window between 2.67 and 2.99 eV. For $CuWO_4$, the MMCT is noticeably lower (2.31 eV) than the Mn, Co, and Ni analogues. This is caused by the significant tetragonal distortion of the octahedral environment around the Cu^{2+} ion (a Jahn–Teller type distortion), which is responsible for lowering the symmetry of the crystal structure to triclinic. This impacts the energy levels of the 3d orbitals on Cu^{2+}, which in turn reduces the energy of the MMCT.

It should be noted that in some prior studies the importance of the 3d orbitals of the A^{2+} ion on the charge transfer transition was recognized, but the LMCT description was retained, and the 3d orbitals were described as altering the energies of the ligand HOMO and metal LUMO.[26,36] Inspection of the PDOS plots for $MnWO_4$ in Figure 6 does reveal some oxygen character in the "Mn 3d" bands, so there is some validity in this description. Nonetheless, the orbital character of the valence bands (or LUMOs) here are predominantly Mn 3d so we feel that the MMCT description paints a more accurate picture.

From the observation that $ZnWO_4$ has a similar charge transfer energy to $MgWO_4$, we can infer that the filled 3d states of the Zn^{2+} do not lie between the O 2p and W 5d sets of bands but rather are located below the highest energy O 2p bands. The PDOS plot for $ZnWO_4$ shown in Figure 7 supports this

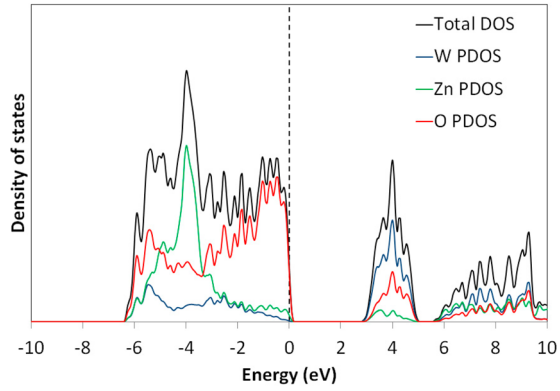

Figure 7. Density of states for $ZnWO_4$. The Fermi energy is shown with a dashed line.

conclusion. The contribution from the Zn 3d orbitals peaks roughly 4 eV below the top of the O 2p bands. Thus, the calculations support the earlier conclusion that the charge transfer for both $MgWO_4$ and $ZnWO_4$ can be described as an LMCT transition from filled O 2p crystal orbitals to antibonding W 5d states.

CONCLUSION

Diffuse reflectance spectra supported by electronic structure calculations of the isostructural AWO_4 series of compounds shed new light on the transitions that impact the color and optical properties of these compounds. Contrary to earlier assumptions, in $MnWO_4$, $CoWO_4$, $NiWO_4$, and $CuWO_4$, the lowest energy charge transfer excitation is a MMCT transition rather than a LMCT transition. The MMCT transition is from

dx.doi.org/10.1021/ic4031798 | Inorg. Chem. 2014, 53, 4394–4399

the partially occupied t_{2g} states of the 3d transition metal ion to the empty W 5d orbitals of the tungstate group. The MMCT energy (2.3−3.0 eV) is considerably lower than the corresponding LMCT energy (3.9−4.1 eV). The presence of a MMCT transition is likely to be a generic feature of salts formed between first row transition metal cations and polyatomic anions such as tungstate, molybdate, and vanadate.

■ ASSOCIATED CONTENT

Supporting Information

X-ray powder diffraction patterns. This material is available free of charge via the Internet at http://pubs.acs.org.

■ AUTHOR INFORMATION

Corresponding Author

*E-mail: woodward@chemistry.ohio-state.edu.

Notes

The authors declare no competing financial interest.

■ ACKNOWLEDGMENTS

The initial studies that inspired this work were carried out by students in Chemistry 123 at The Ohio State University. This work was made possible by the support of the National Science Foundation (Grant CHE-0532250) for the Ohio Research Experiences Enhance Learning (REEL) program. Special thanks to Spencer Porter for assistance with the CASTEP calculations.

■ REFERENCES

(1) Jibril, B. Y. *React. Kinet. Catal. Lett.* **2005**, *86* (1), 171.
(2) Huda, M. N.; Al-Jassim, M. .; Turner, J. A. *J. Renewable Sustainable Energy* **2011**, *3*, No. 053101.
(3) Yourey, J. E.; Pyper, K. J.; Kurtz, J. B.; Bartlett, B. M. *J. Phys. Chem. C* **2013**, *117*, 8708.
(4) Schmitt, P.; Brem, N.; Schunk, S.; Feldmann, C. *Adv. Funct. Mater.* **2011**, *21*, 3037.
(5) Rahimi-Nasrabadi, M.; Pourmortazavi, S. M.; Khalilian-Shalamazari, M. *Proc. INST* **2012**, 1079.
(6) Yan, J.; Shen, Y.; Li, F.; Li, T. *Sci. World J.* **2013**, No. 458106.
(7) Montini, T.; Gombac, V.; Hameed, A.; Felisari, L.; Adami, G.; Fornasiero, P. *Chem. Phys. Lett.* **2010**, *498*, 113.
(8) Zawawi, S. M. M.; Yahya, R.; Hassan, A.; Ekramul Mahmud, H. N. M.; Daud, M. N. *Chem. Cent. J.* **2013**, *7* (80), 2.
(9) Janaky, C.; Rajeshwar, K.; de Tacconi, N. R.; Chanmanee, W.; Huda, M. N. *Catal. Today* **2013**, *199*, 53.
(10) Heyer, O.; Hollman, N.; Klassen, I.; Jodlauk, S.; Bohaty, L.; Becker, P.; Mydosh, J. A.; Lorenz, T.; Khomskii, D. *J. Phys.: Condens Matter.* **2006**, *18*, L471.
(11) Gupta, H. C.; Ruby; Sinha, M. M. *Acta Phys. Pol., A* **2012**, *122*, 142.
(12) Edwin Suresh Raj, A. M.; Mallika, C.; Sreedharan, O. M.; Nagaraja, K. S. *Mater. Lett.* **2002**, *53*, 316.
(13) Sorli, S.; Tena, M. A.; Badenes, J. A.; Llusar, M.; Monrós, G. *Br. Ceram. Trans.* **2004**, *103* (1), 10.
(14) Mikhailik, V. B.; Kraus, H.; Miller, G.; Mykhaylyk, M. S.; Wahl, D. *J. Appl. Phys.* **2005**, *97*, No. 083523.
(15) Mikhailik, V. B.; Kraus, H.; Kapustyanyk, V.; Panasyuk, M.; Prots, Y.; Tsybulskyi, V.; Vasylechko, L. *J. Phys.: Condens. Matter* **2008**, *20*, No. 365219.
(16) Pandey, P. K.; Bhave, N. S.; Kharat, R. B. *J. Mater. Sci.* **2007**, *42*, 7927.
(17) Kim, D. W.; Cho, I.-S.; Shin, S. S.; Lee, S.; Noh, T. H.; Kim, D. H.; Jung, H. S.; Hong, K. S. *J. Solid State Chem.* **2011**, *184*, 2103.
(18) Dunning, N. J.; Megaw, H. D. *Trans. Faraday Soc.* **1946**, *42*, 705.
(19) Kravchenko, V. B. *Zh. Strukt. Khim.* **1969**, *10* (1), 148.
(20) Sleight, A. W. *Acta Crystallogr.* **1972**, *B28*, 2899.
(21) Weitzel, V. H. *Z. Kristallogr.* **1976**, *144*, 238.
(22) Phani, A. R.; Passacantando, M.; Lozzi, L.; Santussi, S. *J. Mater. Sci.* **2000**, *35*, 4879−4883.
(23) Escobar, C.; Cid-Dresdner, H.; Kittl, P.; Dumler, I. *Am. Mineral.* **1971**, *56*, 489.
(24) Filipenko, O. S.; Pobedimskaya, E. A.; Belov, N. V. *Sov. Phys.—Crystallogr.* **1968**, *13*, 163.
(25) Kihlborg, L.; Gebert, E. *Acta Crystallogr.* **1970**, *B26*, 1020.
(26) Ruiz-Fuertes, J.; Lopez-Moreno, S.; Lopez-Solano, J.; Errandonea, D.; Lacomba-Perales, R.; Muñoz, A.; Radescu, S.; Rodriguez-Hernandez, P.; Gospodinov, M.; Nagornaya, L. L.; Tu, C. Y. *Phys. Rev. B* **2012**, *86*, No. 125202.
(27) Lacomba-Perales, R.; Ruiz-Fuertes, J.; Errandonea, D.; Martinez-Garcia, D.; Segura, A. *Europhys. Lett.* **2008**, *83*, No. 37002.
(28) Kubelka, P. *J. Opt. Soc. Am.* **1948**, *38* (5), 448−457.
(29) Kubelka, P.; Munk, F. *Z. Technol. Phys.* **1931**, *12*, 593.
(30) Shapiro, I. P. *Opt. Spektrosk.* **1958**, *4*, 256.
(31) Milman, V.; Winkler, B.; White, J. A.; Pickard, C. J.; Payne, M. C.; Akhmatskaya, E. V.; Nobes, R. H. *Int. J. Quantum Chem.* **2000**, *77*, 895.
(32) Perdew, J. P.; Burke, K.; Ernzerhof, M. *Phys. Rev. Lett.* **1997**, *78*, 1396E.
(33) Naik, S. J.; Salker, A. V. *Solid State Sci.* **2010**, *12*, 2065.
(34) Duffy, A. A. *Bonding, Energy Levels and Bands in Inorganic Solids*; Longman Group: Essex, U.K., 1990.
(35) Blasse, G.; Dirksen, G. J.; Hazencamp, M.; Gunter, J. R. *Mater. Res. Bull.* **1987**, *22*, 813.
(36) Robertson, L. C.; Gaudon, M.; Jobic, P.; Demourges, A. *Inorg. Chem.* **2011**, *50*, 2878.